Ground Penetrating Radar and Microwave Tomography Data Processing for Cultural Heritage: State of Art and Future Trends

Ilaria Catapano, Gianluca Gennarelli, Giovanni Ludeno, Francesco Soldovieri

Istituto per il Rilevamento Elettromagnetico dell'Ambiente, Consiglio Nazionale delle Ricerche

Via Diocleziano 328, 80124 Napoli, Italy

[catapano.i, gennarelli.g, ludeno.g, soldovieri.f]@irea.cnr.it

Abstract

Ground penetrating radar (GPR) is a valuable diagnostic tool for cultural heritage (CH) monitoring and archaeological prospecting applications owing to its ability to inspect optically opaque media and provide information about hidden/buried targets. This article deals with a review of theoretical and practical aspects for an effective and reliable use of GPR in CH applications. Specifically, the focus is on data processing via a linearized microwave tomographic approach. In this context, theoretical and practical issues related to GPR imaging such as clutter and artefacts mitigation as well as three-dimensional reconstruction of large spatial domains are addressed. Finally, an applicative example concerning a survey performed at the Archaeological site of Pompeii, Italy, is presented.

Introduction

Recently, there is an increasing awareness that the management and protection of cultural heritage (CH) is possible only by adopting a holistic approach, which encompasses engineering, physics and social sciences and requires the design and implementation of integrated approaches for CH monitoring. This approach should be multi-scale (from territory monitoring to diagnostics of a single structure and its areas), multi-resolution and able to operate at different investigation depths (i.e. from the surface to the inner of the structures or underground). Significant research examples in this field are reported in the book "Sensing the Past" [1] and subject of recent research H2020 projects as

"Heritages Resilience against Climate Events on Site" (HERACLES, http://www.heracles-project.eu/).

In this context, ground penetrating radar (GPR) is one of the key sensing technologies for in-situ high-resolution diagnostics/prospection of CH assets, since it makes possible imaging the underground (up to depths of some meters) and the inner of structures [2-4].

The application of GPR referred to CH assets is well-assessed as shown in several papers and books [1, 4]. For instance, in the frame of archaeological prospecting, GPR can be deployed as a standalone technology or as a key element of a suite of technologies enabling a multi-scale and multi-resolution investigation, as in the case of the investigation performed in Cahuachi [5]. Noteworthy examples concerning the use of GPR in an integrated approach involving other geophysical techniques are presented in [6-7]. Specifically, the archaeological prospecting at the Roman town of Carnuntum/Austria, which is the largest archaeological landscape in Austria is described in [6]. In this case, the integrated use of aerial imagery and photography and several geophysical techniques such as magnetic, electrical resistivity tomography and GPR was successful in ensuring the high-resolution geometry of the overall site for both the visible and buried structures. Conversely, the localization of the village of Takamatua is discussed in [7]. Here, a complementary combination of horizontal loop electromagnetic, total field magnetic, GPR, and tomographic electrical imaging techniques is presented as a successful case, which allowed the identification of coincident linear anomalous responses supporting the archeological hypothesis about the presence of the blockhouse and its surrounding trench or moat.

Another main application field of GPR deals with CH diagnostics and monitoring, since GPR is able to provide information about the construction modalities and detect possible defects or degradation factors such as voids, fractures, detachments. Representative case studies on the use of GPR for analysing the structural stability of monuments/buildings are reported in [8, 9], where GPR was able to detect voids and fractures in the underground, identify weakness zones in the foundations and walls. A challenging problem for GPR is the investigation of vertical structures such as masonries and

columns. The major difficulty is the presence of layered media, which entails the difficulty to discriminate between the response from the true interfaces and the multiple reflections. In this case, the integration of GPR with sonic prospecting was successful to characterize the deterioration status of pillars in the cathedral of Tricarico (Southern Italy) [10] and allowed the detection of cracks and inhomogeneities in the inner structure of masonry building elements. A good assessment of the capabilities of GPR in masonry monitoring, with a specific focus on columns, is provided in [11].

A GPR system consists essentially of the following subsystems: an electronic unit, a transmitting antenna, a receiving antenna, and a computer [3]. The electronic unit comprises the radar transmitter and receiver. The transmitter generates an ultra-wide-band (UWB) electromagnetic pulse, which is radiated in the ground by the transmitting (Tx) antenna. The electromagnetic wave propagating in the subsurface is reflected/backscattered by the target, and part of the backscattered signal is detected by the receiving (Rx) antenna and converted into an electrical signal. After, this signal is digitized and stored on the computer for visualization and processing. A common feature to any GPR is the capability to measure the two-way travel time between the time instants when the transmitter emits the signal and the backscattered field is collected by the receiver. Specifically, the basic output of any GPR is a trace showing the amplitude of the scattered signal versus two-way travel time for a fixed position of the Tx and Rx antennas (A-scan). By moving the GPR along a measurement line, with a spatial step fixed by the operator according to the antenna working frequency, a B-scan is obtained as the discretized version of a function of two variables, i.e. the measurement position along the horizontal axis and the two-way travel time along the vertical axis. From a B-scan, it is possible to achieve, at least in simple cases, rough information about location and geometry of targets and also to estimate the propagation velocity of the waves into the probed medium [4, 5]. If a 3D reconstruction of the target is required, there is the necessity to survey the area containing it. In particular, several parallel B-scans are needed, possibly gathered along two orthogonal directions, to form a “cube of data” referred as C-scan. A C-scan is the discretized version of a function of three

variables, namely the two spatial coordinates along the measurement surface and two-way travel-time along the vertical axis.

Despite its flexibility and wide diffusion, GPR is a “friendly” technology only when deployed in very simple cases. Indeed, when complex scenarios (as the ones arising in CH applications) are dealt with, raw data interpretability is challenging and advanced data processing techniques must be adopted.

In this frame, Sec. II deals with an advanced data processing approach where the GPR imaging problem is stated in the more general framework of electromagnetic inverse scattering. Specifically, the CH diagnostics problem at hand is formulated as the detection, localization and geometry estimation of a hidden/buried target starting from the field backscattered by the target when illuminated by a known incident field [3, 12, 13]. It is worth noting that the necessity to deploy reliable and computationally efficient imaging approaches pushes towards a simplified electromagnetic modelling. Hence, the attention is focused on linear microwave tomography, which has been proven effective also in real scenarios, as testified by many case studies in other applicative fields [14, 15]. Consequently, Sec. III presents a microwave tomographic approach based on a linearized scattering model. The formulation of the approach is presented under a general scheme, where by changing the relevant key ingredients (incident field and Green’s function), it is possible to deal with complex electromagnetic scenarios beyond the “classical” homogeneous and half-space geometries.

Despite the assessed use of microwave tomography, there are still some practical issues related to clutter and multipath ghosts and to the possibility to achieve 3D images of investigation domains large in terms of the probing wavelength. Section IV summarizes the issues of clutter and ghost artefacts, providing also a brief survey of the related mitigation strategies. Moreover, it accounts for the investigation of large domains and reviews a data processing strategy, based on a pseudo-3D representation of the scene, to reduce the computational burden. Finally, a practical strategy to process massive GPR data is presented. Section V deals with a real case study referred to a GPR survey carried out at the Archaeological site of Pompeii, Italy, in order to provide a practical example of the

potentialities offered by microwave tomography enhanced GPR. Concluding remarks and future trends in GPR for CH monitoring follow in Sec. VI.

Section II. GPR imaging as an inverse electromagnetic scattering

This Section formulates the GPR imaging problem in the frame of the electromagnetic inverse scattering. Indeed, the reconstruction of morphology (location, shape, and size) and electromagnetic features (dielectric permittivity, electrical conductivity and magnetic permeability) of a buried target from its scattered field can be stated as an inverse scattering problem [3, 12, 13]. In principle, the solution of the inverse scattering problem allows for a complete electromagnetic characterization of the investigated scenario if an accurate scattering model of the radar sensing phenomenon is available. The inverse scattering model is derivable from Maxwell's equations in both time and frequency-domain and is commonly presented in terms of a differential or an integral formulation [3, 12, 13].

In order to introduce the inverse scattering problem at hand, let us consider for sake of simplicity the subsurface 2D imaging scenario depicted in Fig. 1, featuring homogeneous, non-dispersive, and non-magnetic media. The upper half-space is air, while the lower half-space is the soil medium characterized by constant relative dielectric permittivity ε_b. The air-soil interface is assumed flat. The scattering phenomenon is activated by a source modelled as a filamentary current polarized along the

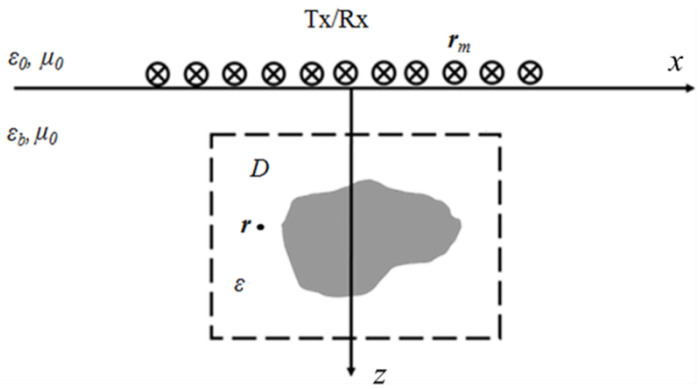

Figure 1. Subsurface sensing scenario

y-axis (TM polarization) and radiating an electromagnetic signal. The $\exp(j\omega t)$ time dependence is assumed, with $\omega = 2\pi f$ being the angular frequency and f belonging to the frequency range $[f_{min}, f_{max}]$. The source and measurement points, i.e. the location where the scattered field is collected, are located at the air-soil interface and their horizontal offset is supposed to be negligible. Hence, the scattering model is defined under a multi-monostatic/multi-frequency measurement configuration. Let D be the probed domain, i.e. the spatial region where the target is located, $\boldsymbol{r}$ the generic point in D, and $\chi = \frac{\varepsilon}{\varepsilon_b} - 1$ the contrast function accounting for the variation of the unknown target dielectric permittivity, ε, with respect to the one of the investigated medium.

For each measurement position $\boldsymbol{r}_m$ and angular frequency ω, the scattering phenomenon is described by the pair of scalar integral equations [4, 12]

$$e_s(\boldsymbol{r}_m, \omega) = k_b^2 \iint_D g_e(\boldsymbol{r}_m, \boldsymbol{r}, \omega) e_{tot}(\boldsymbol{r}, \omega) \chi(\boldsymbol{r}) d\boldsymbol{r} \quad (1)$$

$$e_{tot}(\boldsymbol{r}, \omega) = e_{inc}(\boldsymbol{r}, \omega) + k_b^2 \iint_D g_i(\boldsymbol{r}, \boldsymbol{r}', \omega) e_{tot}(\boldsymbol{r}', \omega) \chi(\boldsymbol{r}') d\boldsymbol{r}' \quad \boldsymbol{r} \in D \quad (2)$$

where k_b is the wave-number in the soil. Bold fonts used in eqns. (1) and (2) denote vector quantities. Equation (1) provides the field e_s scattered by the target (the datum of our problem), which can be seen as the field radiated by the equivalent "source" defined by the product of the unknown contrast function χ and of the total field e_{tot} in D. The total field is defined by eqn. (2) and is given by the sum of the incident field e_{inc}, i.e. the field in D when the targets are absent and a second contribution, defined as an integral on D, which accounts for the mutual interactions occurring in D. The quantities g_e and g_i are the 'external' and 'internal' Sommerfeld-Green's functions, respectively [3, 13]. The 'external' Sommerfeld-Green's function g_e accounts for the field generated at $\boldsymbol{r}_m$ by the elementary source located at $\boldsymbol{r} \in D$. Conversely, the "internal" Sommerfeld-Green's function g_i expresses the field generated at $\boldsymbol{r} \in D$ by an elementary source placed at $\boldsymbol{r}' \in D$.

It is worth noting that eqns. (1) and (2) provide a unified frame suitable to account for different scenarios and measurement configurations, once the proper expressions for the incident field and the Sommerfeld-

Green's functions are accounted for. These quantities depend on geometry and electromagnetic properties of the reference scenario as well as on the adopted measurement configuration [13].

Solving an inverse scattering problem means that the coupled eqns. (1) and (2) have to be jointly inverted and this task involves significant mathematical difficulties. The first one is related to the non-linearity of the relationship between the unknown contrast function and the scattered field. Indeed, the scattered field is linearly related to the product of the total field e_{tot} and the contrast function χ (see eqn. (1)), but the total field depends on the contrast function through eqn. (2). As a result, a non-linear relationship exists between data and unknown and false solutions (local minima) arise if the inverse scattering problem is solved without any approximation and using local optimization procedures [16]. Indeed, most solution approaches formulate the inverse problem as the search of the global minimum of a cost functional. Accordingly, global optimization strategies should be adopted to ensure the optimality of the solution. Since a global optimization involves often an unfeasible computational burden, it is common to use local optimization procedures. These last are efficient from the computational viewpoint but can be trapped into local minima providing a false solution [16].

A further difficulty in achieving reliable quantitative reconstructions is the lack of an accurate knowledge of the relevant Sommerfeld-Green's functions in practical cases. Indeed, based on eqns. (1) and (2), it is necessary to know the field radiated by a real antenna in a layered medium, which is a very challenging problem. For those reasons, at best authors' knowledge, the experimental validation of exact inverse scattering approaches has been limited only to simplified cases, e.g. laboratory tests by assuming a free-space scenario and antennas located far from the investigated objects [17]. Of course, these conditions are far from those arising when performing GPR surveys for CH monitoring.

Section III. The linear inverse scattering approach as a reliable solution tool for GPR imaging

A notable simplification of the problem is achieved by invoking the Born approximation [3], which amounts to consider the total field in eqn. (1) equal to the incident field or, in other words, to neglect the integral

term appearing at the right hand side of eqn. (2). From a physical viewpoint, Born approximation implies that the mutual interactions occurring into the investigation domain are negligible. Accordingly, when Born approximation is used, no quantitative reconstruction of the target is possible unless targets are weak scatterers, i.e. they are a small perturbation with respect to the host medium. Despite that, it has been observed that the use of the Born approximation based formulation of the inverse scattering problem allows detection, localization and rough estimation of the geometry of the targets [8-10].

According to the Born approximation, the unknown–data relationship is given by the following Fredholm integral equation:

$$e_s(\boldsymbol{r}_m, \omega) = k_b^2 \iint_D g_e(\boldsymbol{r}_m, \boldsymbol{r}, \omega) e_{inc}(\boldsymbol{r}, \omega) \chi(\boldsymbol{r}) d\boldsymbol{r} = L(\chi) \tag{3}$$

where L denotes the linear radiation operator, whose kernel is given by the product between the external Sommerfeld-Green's function g_e and the incident field e_{inc}. Note that the operator L relates directly the unknown contrast function to the scattered field. Therefore, the reconstruction of the contrast function is carried out through the inversion of eqn. (3), which involves still some mathematical difficulties owing to the ill-posedness of the linear inverse problem [18]. Indeed, L is a compact operator and this entails that a solution of the problem may not exist and does not depend continuously on data, as deeply discussed in [18]. From the practical viewpoint, this means that due to the unavoidable noise on data, only a finite accuracy representation of the scenario under test can be obtained. The lack of existence and stability of solution can be remedied by introducing a regularization scheme [18]. Anyway, the necessity to regularise the inverse problem introduces a spatial filtering of the retrievable components of the unknown [3, 19].

The regularization of the inverse problem is herein carried out by resorting to the Truncated Singular Value Decomposition (TSVD) tool. More precisely, after eqn. (3) has been discretized, the imaging task amounts to solve the matrix inverse problem:

$$\mathbf{e}_s = \mathbf{L}\boldsymbol{\chi} \tag{4}$$

where $\mathbf{e}_s$ is the $K = M \times F$ dimensional data vector, M being the number of spatial measurement points and F the number of frequencies, $\boldsymbol{\chi}$ is the $N_p$dimensional unknown vector, N_p being the number of points in D, and $\mathbf{L}$ is the $K \times N_p$ dimensional matrix obtained by discretizing the integral operator. Since matrix $\mathbf{L}$ stems from discretization of an ill-posed integral equation, inversion of $\mathbf{L}$ is an ill-conditioning problem, which means that the solution is very sensitive to measurement uncertainties and noise on data. Hence, a regularization scheme has to be applied to obtain a robust and physically meaningful solution. One possibility in this sense is the Truncated Singular Value Decomposition (TSVD) scheme [18]:

$$\tilde{\boldsymbol{\chi}} = \sum_{n=1}^{H} \frac{\langle \boldsymbol{E}_s, \boldsymbol{u}_n \rangle}{\sigma_n} \boldsymbol{v}_n \tag{5}$$

In eqn. (5) $\langle \cdot, \cdot \rangle$ denotes the scalar product in the data space, H is a truncation index, $\{\sigma_n\}_{n=1}^{Q}$ is the set of singular values of the matrix $\mathbf{L}$ ordered in a decreasing way, $\{\boldsymbol{u}_n\}_{n=1}^{Q}$ and $\{\boldsymbol{v}_n\}_{n=1}^{K}$ are the right and left sets of the singular vectors in data and unknown spaces, respectively. The index $H \leq Q$ ($Q = \min\{K, N_p\}$) sets the "degree of regularization" of the solution and is chosen in such a way to find a trade-off between the accuracy and resolution requirements from one side (which pushes to increase H) and solution stability from the other side (which pushes to reduce H).

The imaging result is given as the spatial map of the modulus of the retrieved contrast vector $\tilde{\boldsymbol{\chi}}$ normalized to its maximum value in the scene. Hence, the regions of D where the modulus of $\tilde{\boldsymbol{\chi}}$ are significantly different from zero are representative of the position and geometry of the targets.

Section IV. Practical issues in the application of microwave tomography for CH applications

Besides the mathematical difficulties pointed out in the previous Section, additional GPR imaging issues arise in operative scenarios typical of archaeological prospecting and CH diagnostics. These scenarios are usually very challenging because of clutter and mutual interactions among targets as well as the requirement of 3D images from which one can identify the geometrical features of the targets located at different depths. This section aims at reviewing briefly these issues and the proposed strategies to face them and provides a convenient strategy to process large-scale GPR data.

Clutter

The term clutter refers to all those unwanted signals that are not backscattered by the targets and are recorded in the acquisition time window [1, 2, 3]. A major source of clutter is the direct coupling between the transmitting and receiving antennas. UWB transmitting and receiving antennas are commonly shielded in the same box, and thus, a significant part of the electromagnetic signal propagates from the transmitter to the receiver directly, i.e., without interacting with the targets. Such a signal may completely obscure the field backscattered by shallow targets and then prevent their detection. As a consequence, the effectiveness of GPR surveys is strongly related to the capability of removing the direct coupling signal from the raw data without distorting excessively the field scattered by the targets, because this would seriously affect the interpretation of the results. The "ideal clutter removal" procedure consists in subtracting from the total field (the signal contribution accounting for targets and background) the field in absence of targets (the background signal). However, in realistic cases, background measurements are not available or very difficult to achieve. Accordingly, unconventional hardware solutions or a suitable signal processing must be adopted.

In the framework of hardware solutions, it is worth mentioning the differential GPR system [20], where the differential signal is achieved directly during the survey as the difference between the signals collected by two receiving antennas located at the same height above the air-soil interface and arranged symmetrically with respect to the transmitting antenna. However, it has been observed and theoretically shown that this configuration badly affects the reconstruction performance, since it introduces a filtering of the low spatial variations of the targets [21].

The second class of methods exploits clutter filtering procedures in time or frequency domain. A very simple filtering approach is commonly referred as time-gating and amounts to erase the early time response of the received signal [2, 3]. However, the automatic selection of the time window wherein the signal must be "silenced" is an open issue, which becomes particularly critical for shallow targets. Other popular filtering approaches are based on the assumption that the ground response is slowly spatially

varying (as compared to localized scatterers) along the antenna movement direction. In particular, the background removal consists in replacing the current A-scan with the difference between it and the average value of all the A-scans that compose the B-scan (or a subset of A-scans close to the trace of interest). This operation erases all the flat interfaces present in the data (including the air-soil interface) and usually provides a cleaner image of the buried scenario. However, this spatial filtering also acts on the field scattered by the target and therefore compensation procedures are required to restore the point spread function [22].

In the frame of ground clutter filtering, it is also worthwhile to mention the subspace projection method [23]. For this approach, the clutter signal is assumed much stronger than the target one and accordingly its contribution is related to the highest singular value of the raw data matrix. Therefore, once the SVD of the data matrix has been computed, the gathered data are projected on the subspace spanned by the singular vectors related to the singular values different from the largest ones. The main drawback of this method is the estimation of the clutter subspace dimension, which is usually made based on a visual inspection of the singular values of the data matrix. An alternative filtering approach, the entropy-based time-gating has been proposed in [24]. This method performs an automatic selection of the time-gating window on the basis of an entropy criterion. This allows, in principle, not only to eliminate the clutter due to the air-soil interface but even the other undesired signals (due to multiple reflections), by avoiding an unwanted filtering of the target.

Mutual interactions

In real applications such as CH diagnostics, the radar signal is composed by the direct scattered fields as well as multipath contributions, which account for the mutual interactions among targets and the background scenario. However, the commonly adopted radar imaging approaches are based on simplified and approximated models of the electromagnetic scattering phenomena, such as that defined by eq. (3), which only account for the direct scattered fields while neglecting the occurrence of multipath

contributions. Because of this approximation, GPR images may become difficult to be reliably interpreted because they are often affected by false targets (ghosts) located at positions where no physical target exists. In this context, multipath ghost suppression becomes very important to enhance the interpretability of the images. Several approaches have been developed, under far-field conditions and free-space case, by exploiting the aspect-dependent character of multipath ghosts by sub-aperture imaging strategies [25, 26] or the nonlinearity of the phase delays of ghosts in the data [27]. In [25], the problem is faced for the more realistic case of targets located in the near-field zone of the radar, which is a typical operation condition for GPR surveys. The study has shown that multipath ghosts can be suppressed by properly selecting the measurement set-up and applying a suitable image fusion strategy. Specifically, the key idea is to combine the reconstructions achieved with subarray configurations in monostatic and single view/multistatic mode by means of simple arithmetical (additive and multiplicative) image fusion operations. The multiplicative subarray image fusion (MSIF) approach has been also compared with the popular coherence factor (CF) filtering technique, which mitigates clutter by suppressing its low-coherence features [28]. The result of this comparison has shown that both MSIF and CF are robust to noise and have similar detection performance [29]. More in detail, MSIF notably improves the imaging quality, yielding lower clutter than CF filtering; however, it attenuates also the response of the targets as the number of subarrays increases and so it tends to suppress weaker targets. On the other hand, if a constant false alarm detection scheme is implemented over the filtered images, the same detection performance are provided by MSIF and CF filtering, so both methods can be equivalently exploited to enhance target detectability in highly cluttered environments. Despite the encouraging results, further work is still necessary to develop automatic procedures able to deal with large investigation domains.

3D imaging

Another main aim in GPR imaging is to provide 3D images of investigation domains that are usually very

large in terms of the probing wavelength. For such domains, the application of well-assessed full-3D imaging approaches [3, 14] is unusual because of the practical feasibility of the survey and the high computational burden involved in the inversion process. In this case, the most common way to avoid the computational issue is to determine a pseudo 3D representation of the investigated domain. More in detail, the inversion algorithm is based on two steps. In the first step, 2D sections of the investigation domain are achieved by processing the single B-scans data; after, these 2D sections are superimposed and interpolated to achieve the pseudo 3D representation of the investigation domain. The method provides reliable reconstructions in the case of elongated targets, as buried road or walls; conversely, the performance worsens in the case of localized objects [3, 13]. Actually, the field scattered by a localized target is collected not only on the profile passing above the object but also on the closer scanning lines. Therefore, when the 2D reconstructions are superimposed the target is seen as an "elongated object" along the direction orthogonal to the one of the profiles (see [4, 15] for a comparison between the full-3D and pseudo 3D approaches). Note that a possible strategy to mitigate this issue is to collect the GPR data also along orthogonal profiles and after apply image fusion procedures similar to those presented for multipath suppression [30].

In conclusion, a convenient strategy to process large scale GPR data collected on a plane is the following one:

1. 2D tomographic reconstructions along each B-scan (profile) through the two steps:
   1.1 Application of clutter removal procedures (mainly to suppress direct coupling between the antennas and reflection from the air/soil interface)
   1.2 Application of multipath mitigation strategies
2. Pseudo 3D representation

Alternatively, on small areas of the investigation domain, a full 3D imaging approach [3] can be applied to achieve a reconstruction of small/localised objects.

Section V. Validation

As an example assessing the imaging capabilities of the microwave tomography enhanced GPR, let us consider the survey performed at the Roman Amphitheater located in the south-west part of the archeological site of Pompeii. A 20.4 m x 9 m wide area of the underground of the amphitheater was investigated. This area was located close to a temporary installation present at the time of the measurement campaign (see Figure 2).

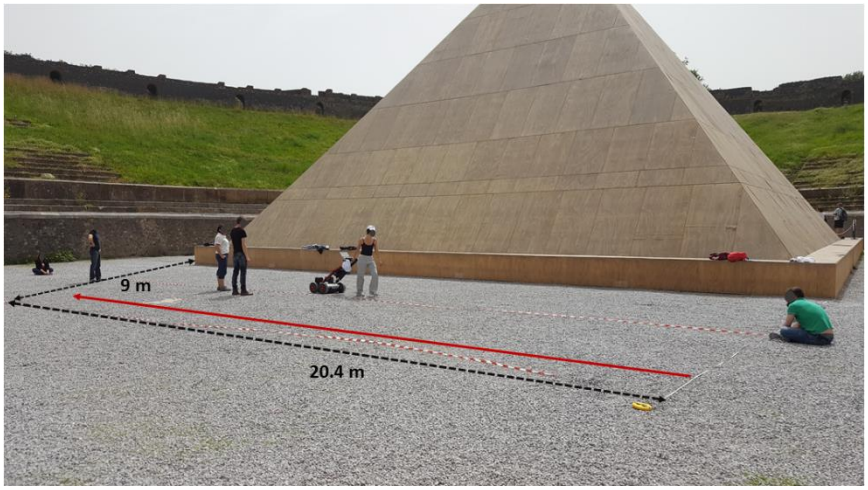

Figure 2. Investigated area of the Roman Amphitheater at the Pompeii archaeological site

Specifically, data were gathered along 19 parallel profiles with a spacing of 0.5 m and oriented as the red arrow in Figure 2. The radar used for the surveys was the IDS K2-RIS GPR system equipped with a dual frequency shielded antenna whose nominal central frequencies are f_{c1} = 200 MHz and f_{c2} = 600 MHz; here, we consider the dataset collected at f_{c1} = 200 MHz. The data were recorded with a 0.035 m spatial offset along the measurement line and the observation time window was fixed at 120 ns. After zero time setting at 8 ns, the background removal was applied to filter out the direct coupling of the antenna and the signal due to the air-soil interface. Figure 3 compares raw and filtered data referred to one of the gathered profiles in order to show the effect of the above pre-processing procedures.

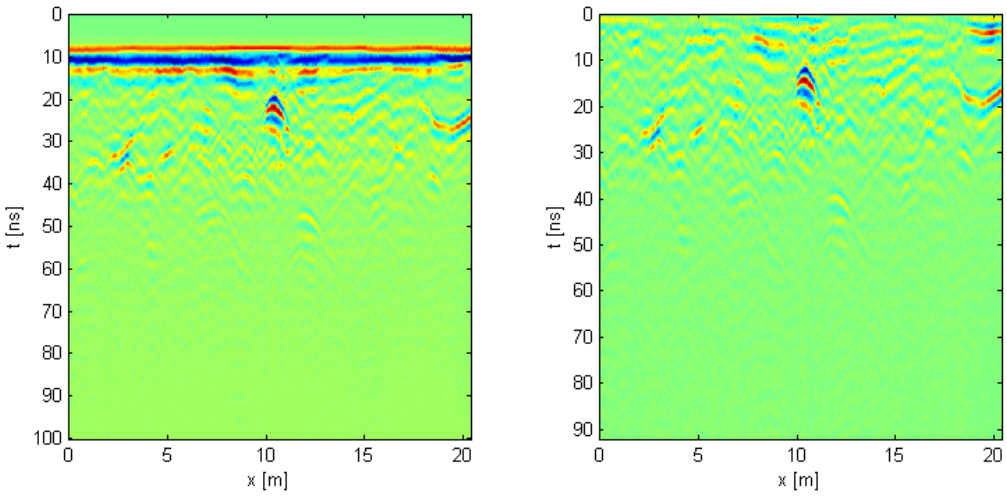

Figure 3: Comparison between raw data (left panel) and filtered data by means zero time correction and background removal (right panel).

The 2D microwave tomographic approach (MWT) was applied as described in Section III on the single profiles (B-scans). In this frame, the frequency range from 150 MHz to 400 MHz was selected as useful spectrum of the data and was evenly sampled by 11 frequencies, i.e. the frequency spacing was fixed at 10 MHz. The relative dielectric permittivity of the background was assumed equal to 9 and each 2D tomographic inversion was regularized by setting the TSVD threshold in such a way to filter out all the singular values that are 30 dB lower than the maximum one. In this way, 19 2D tomographic images were achieved, which were combined to obtain the pseudo 3D representation of the volume under investigation. The results of the MWT data processing are shown in Figure 4, which shows the retrieved contrast as normalized to its maximum value into the overall spatial volume under test and at constant depth slices. As can be seen, the images in Figure 4 reveal the presence of an elongated structure at depth z= 0.6 m, ranging from y = 0 m to y =9 m and centered at x=10 m, which could be attributed to a water duct maybe built during previous restoration works. Moreover, several anomalies appear at depth ranging from z = 0.9 m to z = 1.8 m but their interpretation is still an open issue that is under discussion with the archeologists. In particular, two circulars structure appears, one

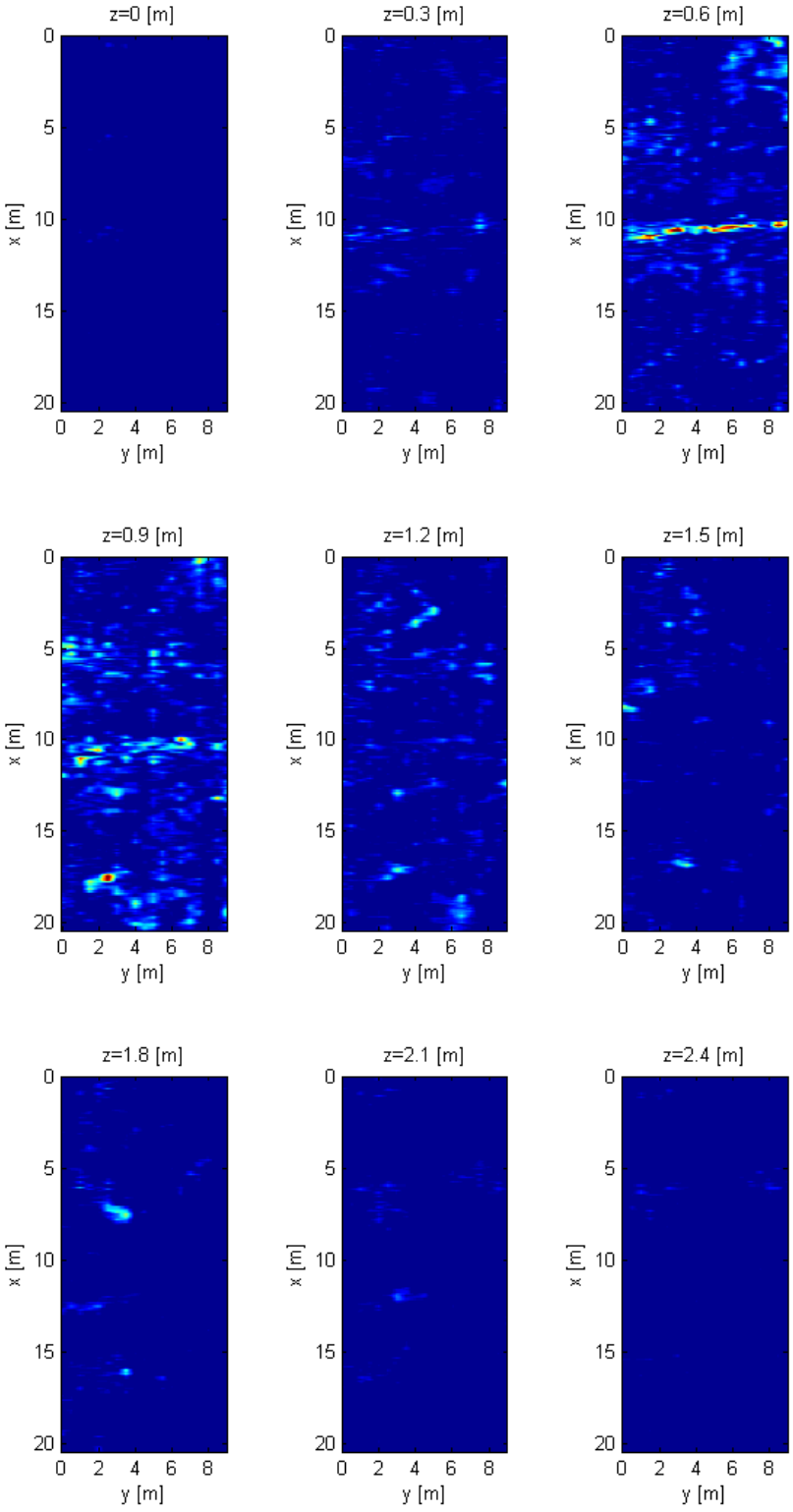

Figure 4: Tomographic images at increasing constant depth values

located at z = 0.6 m in the upper right corner and one at z = 0.9, for x ranging from about 17 m to 20 m and y from about 2 m to 7 m.

Finally, a comparison of the imaging capabilities of MWT approach with those provided by two commonly adopted imaging strategies, specifically adjoint inversion (ADJ) and delay and sum (DAS) strategy [2, 15, 18], is given in Figure 5. This latter shows depth slices at z = 0.6 m, 0.9 m and 1.2 m obtained by applying MWT (upper panels), ADJ (middle panels) and DAS (lower panels). By observing Figure 5, one can note that MWT and DAS provide comparable results, even if MWT allows a better identification of the spatial distribution of the retrieved anomalies. In addition, ADJ provides worse performance especially at increasing depths, where the anomalies are progressively missed.

Section VI. Conclusion and perspectives

The paper has provided an overview of the main theoretical and practical aspects of GPR imaging for CH monitoring applications by focusing on a linear microwave tomographic approach and accounting for strategies devoted to reduce artefacts and provide effective 3D images of the scenario under test. An applicative example concerning a survey performed in the Roman amphitheater of the Pompeii archaeological site has been presented as a test case to assess the effectiveness, in terms of image interpretability, of the considered approach.

Despite the advances in GPR technology and signal processing algorithms, some challenges still have to be faced for a successful application of GPR in operative conditions.

The first one is the development of hardware solutions capable to: i) speed-up the surveys; ii) improve the radar performance in terms of sensitivity and clutter rejection; iii) allow for innovative measurement configurations to mitigate clutter.

As regards large-scale surveys, the need for portability should be conjugated with the possibility of using antenna arrays for multiple data acquisitions. In this respect, the adoption of antenna arrays able to implement in real-time measurement configurations different from the monostatic one (e.g.

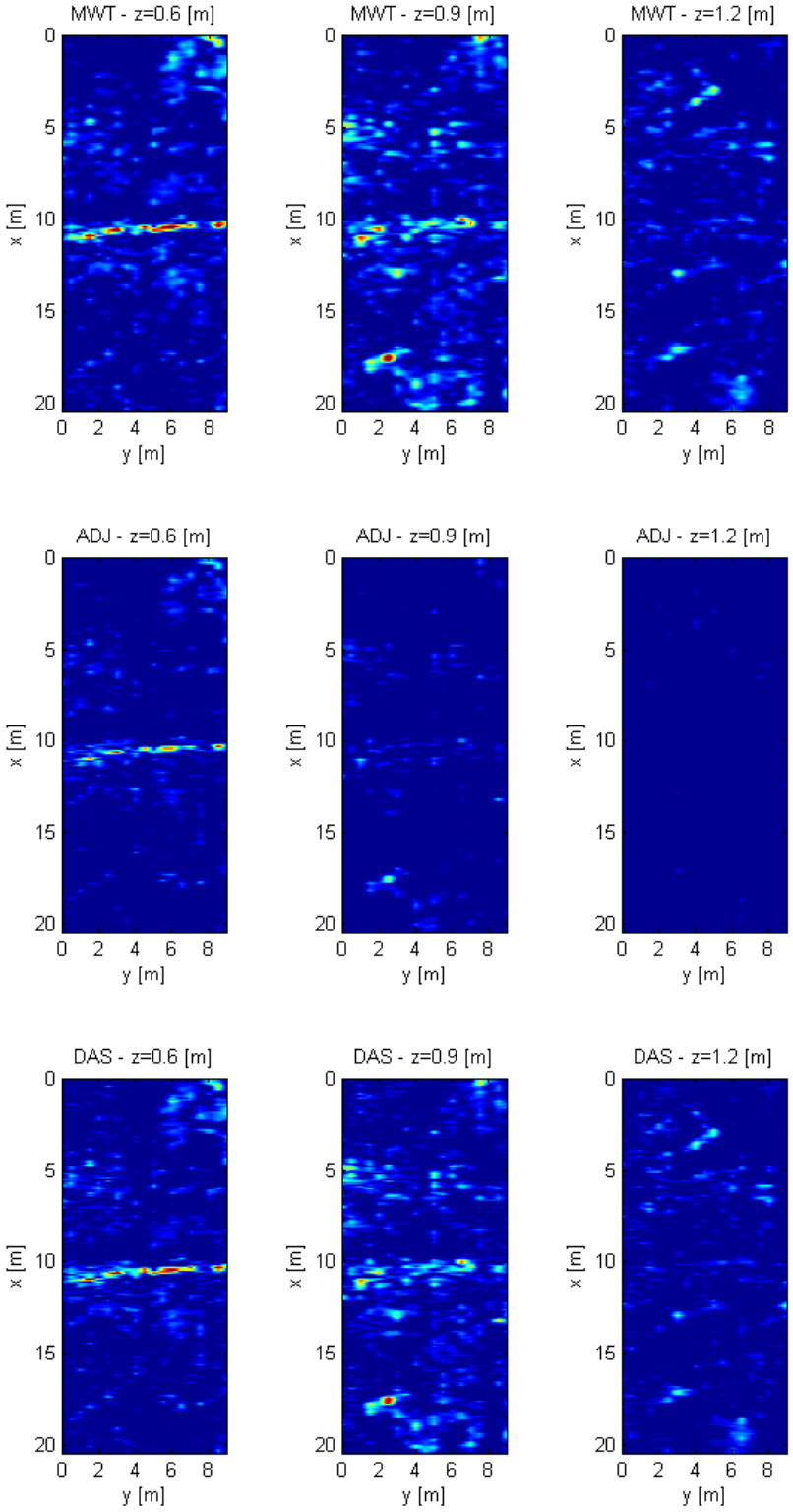

Figure 5: Comparison of the depth slices at z = 0.6 m , 0.9 m, 1.2 m reconstructed by means of MWT (upper panels), ADJ (middle panels) and DAS (lower panels).

multi-view/multi-static/multi-polarization) would allow to enrich the data information and improve the quality of target reconstructions. Of course, this implies the development of ad hoc strategies capable of managing multi-view/multi-static/multi-polarization data in order to exploit properly the information diversity that this kind of data provide, while keeping feasible the computational burden in terms of memory requirements and computational time.

Furthermore, recent advances are concerned with the development and experimentation of GPR systems mounted on airborne, helicopter or UAV platforms. In this context, research activities are starting to address the development of effective approaches able to integrate navigation data, provided by global positioning systems and inertial navigation sensors, with radar data in order to manage arbitrary measurement trajectories different from ideal straight lines and/or to correct motion deviations commonly occurring with respect the planned flight path. Moreover, the possibility to consider curved and rough air-soil interfaces represent an opportunity of future research work.

Finally, the adoption of advanced electromagnetic models, capable of describing accurately the signal radiated into the investigated medium as well as of accounting for the signal propagation into complex scenarios, represent a constantly active research activity, which is essential to move from qualitative to quantitative reconstructions of the scenarios under test.

Acknowledgment: The authors thank Dr. Bruno De Nigris and Marialaura Iadanza of the “Parco Archeologico di Pompei” for providing the permission and support to the logistics of GPR surveys carried out in the Amphiteather.

References

1. N. Masini and F. Soldovieri.*Sensing the Past*. Springer, 2017.
2. D. J. Daniels*. Ground Penetrating Radar*. John Wiley & Sons, 2005.
3. R. Persico, *Introduction to ground penetrating radar: inverse scattering and data processing*. John

Wiley & Sons, 2014.

4. L. B. Conyers. *Ground Penetrating Radar for Archaeology*. AltaMira Press, 2004
5. R. Lasaponara, N. Masini, E. Rizzo, G. Orefici, “New discoveries in the Piramide Naranjada in Cahuachi (Peru) using satellite, Ground Probing Radar and magnetic investigations”, *Journal of Archaeological Science*, vol. 38, pp. 2031-2039, 2011
6. W. Neubauer, C. Gugl, M. Scholz, G. Verhoeven, I. Trinks, K. Löcker, M. Doneus, T. Saey, and M. Van Meirvenne, “The discovery of the school of gladiators at Carnuntum, Austria”, *Antiquity*, vol. 88, no. 339, pp. 173-190, 2014.
7. D.C. Nobes, L.R. Wallace, “Geophysical imaging of an Early nineteenth century colonial defensive blockhouse: applications of EM directionality and multi-parameter imaging”, In: El-Qady G., Metwaly M. (eds) Archaeogeophysics. Natural Science in Archaeology. Springer, Cham, pp. 219-232, 2019.
8. S. Kadioglu, Y. K. Kadioglu, I. Catapano, F. Soldovieri, “Ground penetrating radar and microwave tomography for the safety management of a cultural heritage site: Miletos Ilyas Bey Mosque (Turkey)”, *Journal of Geophysics and Engineering*, vol. 10, no. 6, pp. 064007, 2013.
9. I. Catapano, G. Ludeno, F. Soldovieri, F. Tosti, G. Padeletti, “Structural Assessment via Ground Penetrating Radar at the Consoli Palace of Gubbio (Italy),” *Remote Sensing*, vol. 10, no. 1, pp. 45, 2017.
10. G. Leucci, N. Masini, R. Persico, F. Soldovieri, “GPR and sonic tomography for structural restoration: the case of the cathedral of Tricarico,” *Journal of Geophysics and Engineering*, vol. 8, no. 3, 2011
11. S. Santos-Assuncao, V. Perez-Gracia, O. Caselles, J. Clapes, V. Salinas, “Assessment of complex masonry structures with gpr compared to other non-destructive testing studies,” *Remote Sensing*, vol. 6, no. 9, pp. 8220–8237, 2014.
12. M. Pastorino. *Microwave imaging*. vol. 208, John Wiley & Sons, 2010.

13. W. C. Chew, *Waves and fields in inhomogeneous media*. Institute of Electrical and Electronics Engineers, Piscataway, N.J., 1995.
14. T. B. Hansen and P. M. Johansen, “Inversion scheme for ground penetrating radar that takes into account the planar air-soil interface,” *IEEE Trans. Geosci. Remote Sens.*, vol. 38, no. 1, pp. 496-506, 2000.
15. R. Solimene, I. Catapano, G. Gennarelli, A. Cuccaro, A. Dell'Aversano, and F. Soldovieri, “SAR imaging algorithms and some unconventional applications,” *IEEE Signal Process*. *Mag*., vol. 31, no. 4, pp. 90–98, 2014.
16. T. Isernia, V. Pascazio, and R. Pierri, “On the local minima in a tomographic imaging technique”, *IEEE Trans. Geosci. Remote Sens*., vol. 39, no. 7, pp. 1596-1607, 2001.
17. J. M. Geffrin and P. Sabouroux, “Continuing with the Fresnel database: experimental setup and improvements in 3D scattering measurements”, *Inverse Problems*, vol. 25, no. 2, pp. 024001, 2009.
18. M. Bertero and P. Boccacci. *Introduction to inverse problems in imaging*. Institute of Physics Publishing, Bristol and Philadelphia, 1998.
19. R. Persico, R. Bernini, and F. Soldovieri, “The role of the measurement configuration in inverse scattering from buried objects under the Born approximation,” *IEEE Trans. Antennas Propag.*, vol. 53, no. 6, pp. 1875-1887, 2005.
20. R. Persico, G. Pochanin, V. Ruban, A. Orlenko, I. Catapano, F. Soldovieri, “Performances of a microwave tomographic algorithm for GPR systems working in differential configuration”, *IEEE Journal of Selected Topics in Applied Earth Observations and Remote Sensing*, vol. 9, no. 4, pp. 1343-1356, 2016.
21. R. Persico and F. Soldovieri, A Microwave tomography approach for a differential configuration in GPR prospecting, *IEEE Trans. Antennas Propag.*, vol. 54, no. 11, pp. 3541-3548, 2006.
22. R. Persico and F. Soldovieri, “Effects of background removal in linear inverse scattering,” *IEEE Trans. Geosci. Rem. Sens.,* vol., no. 4, pp. 1104-1114, 2008.

23. M. Garcia-Fernandez, Y. Alvarez-Lopez, A. Arboleya-Arboleya, F. Las-Heras, Y. Rodriguez-Vaqueiro, B. Gonzalez-Valdes, A. Pino-Garcia, "SVD-Based clutter removal technique for gpr", *IEEE International Symposium on Antennas and Propagation & USNC/URSI National Radio Science Meeting*, pp. 2369-2370, 2017.

24. R. Solimene, A. Cuccaro, A. Dell'Aversano, I. Catapano, F. Soldovieri, "Ground clutter removal in GPR surveys," *IEEE Journal of Selected Topics in Applied Earth Observations and Remote Sensing*, vol. 7, no. 3, pp. 792-798, 2014.

25. D. Obuchon, D. Garren, J. S. Goldstein, R. Greene, J. North, "Drift inversion estimation of multipath ghosts in sar image reconstruction," Proc. IEEE Radar Conference, April 2004, pp. 556–558.

26. G. Gennarelli and F. Soldovieri, "Multipath ghosts in radar imaging: physical insight and mitigation strategies", *IEEE Journal of Selected Topics in Applied Earth Observations and Remote Sensing*, vol. 8, no. 3, pp. 1078-1086, 2015.

27. J. DeLaurentis, "Multipath synthetic aperture radar imaging," Radar, Sonar Navigation, IET, vol. 5, no. 5, pp. 561–572, 2011.

28. R. J. Burkholder and K. E. Browne, "Coherence factor enhancement of through-wall radar images," *IEEE Antennas Wireless Propag. Lett*., vol. 9, pp. 842–845, 2010.

29. G. Gennarelli, G. Vivone, P. Braca, F. Soldovieri, M. G. Amin, "Comparative analysis of two approaches for multipath ghost suppression in radar imaging," *IEEE Geosci. Rem. Sens. Lett.*, vol. 13, no. 9, pp. 1226-1230, 2016.

30. F. Soldovieri, R. Solimene, F. Ahmad, "Sparse tomographic inverse scattering approach for through-the-wall radar imaging", *IEEE Trans. Instrum. Meas.*, vol. 61, no. 12, pp. 3340-3350, 2012.